A Piezoelectric Unimorph Deformable Mirror Concept by Wafer Transfer for Ultra Large Space Telescopes

Eui-Hyeok Yang and Kirill Shcheglov

MEMS Technology Group, In Situ Technology and Experiments Systems Section,
Jet Propulsion Laboratory, California Institute of Technology
4800 Oak Grove Drive, Pasadena, CA 91109
Eui-Hyeok.Yang@jpl.nasa.gov ph: +1-818-354-7059 fx: +1-818-393-6047

ABSTRACT

Future concepts of ultra large space telescopes include segmented silicon mirrors and inflatable polymer mirrors. Primary mirrors for these systems cannot meet optical surface figure requirements and are likely to generate over several microns of wavefront errors. In order to correct for these large wavefront errors, high stroke optical quality deformable mirrors are required. JPL has recently developed a new technology for transferring an entire wafer-level mirror membrane from one substrate to another. A thin membrane, 100 mm in diameter, has been successfully transferred without using adhesives or polymers. The measured peak-to-valley surface error of a transferred and patterned membrane (1 mm x 1 mm x 0.016 mm) is only 9 nm. The mirror element actuation principle is based on a piezoelectric unimorph. A voltage applied to the piezoelectric layer induces stress in the longitudinal direction causing the film to deform and pull on the mirror connected to it. The advantage of this approach is that the small longitudinal strains obtainable from a piezoelectric material at modest voltages are thus translated into large vertical displacements. Modeling is performed for a unimorph membrane consisting of clamped rectangular membrane with a PZT layer with variable dimensions. The membrane transfer technology is combined with the piezoelectric bimorph actuator concept to constitute a compact deformable mirror device with a large stroke actuation of a continuous mirror membrane, resulting in a compact AO systems for use in ultra large space telescopes.

Keywords: Deformable mirror (DM), Microelectromechanical Systems (MEMS), Adaptive optics, Piezoelectric actuator, Unimorph actuation, Continuous mirror, Wafer-level membrane transfer, Segmented Space Telescope

1. INTRODUCTION

Precision deformable mirrors are key components for high-contrast imaging instruments such as large segmented telescopes. The strong need of deformable micromirrors exists for high spatial frequency wavefront error correction. Active wavefront control subsequent to reflection from the primary mirror is needed, particularly to overcome the potential large spatial frequency errors.

An electrostrictive lead magnesium niobate (PMN) technology has been successfully demonstrated with an excellent surface stability of 1 angstrom and a surface figure of $\lambda/20$ [1]. Other materials such as super piezoelectric (PMN-PT) and lead zirconium titanate (PZT) ceramics have been developed for this application. Also, some of these other materials have been shown to possess good cryogenic properties. However, although these technologies are in widespread use, they are still limited by the actuator stroke per pixel density (approx. 0.5 μm stroke for 1/mm^2 density for PMN-based mirrors). Therefore, it would be a significant improvement in technology if an optical quality mirror with a higher pixel density could be fabricated, while maintaining the required actuator stroke.

Recently, the use of advanced Micro Electro Mechanical Systems (MEMS) technology has been shown to reduce the mass and volume of the optical device by several order-of-magnitude over conventional technologies. The key challenge remains to demonstrate optical quality micromirrors with this technology, which, if shown to be possible, will enable the design of smaller optical systems without loss of capability. Although segmented mirrors have been fabricated with individual pixel tip/tilt capability [2-4], a continuous surface figure is required to increase the imaging sensitivity. Micromachined continuous membrane deformable mirrors have also been fabricated [5-8]. However, the devices fabricated using these approaches often result in limited actuator stroke and/or marginal surface quality [7]. Compact, high stroke deformable mirrors need to be developed for the aberration compensation of future Large Lightweight Segmented or Inflatable Space Telescopes.

We report, in this paper, a piezoelectric deformable mirror technology based on transferred optical quality membranes in order to meet the demanding requirements for optical quality and mechanical compliance.

2. UNIMORPH DEFORMABLE MIRROR

The deformable mirror device in this paper consists of a transferred continuous membrane mirror supported by a unimorph actuator array as shown in Figure 1. This novel actuator geometry makes it possible to have low inter-actuator coupling and a quality mirror surface. The approach also has the flexibility of allowing different actuation mechanisms to be incorporated with the membrane transfer technology. This work focuses on developing modeling and process technologies for fabricating and integrating high stroke actuators with the mirror transfer technique. The appropriate control mechanism for the actuator array is necessary to be addresses, but it is beyond the scope of this paper. The scalability issue, namely, how to maintain the surface quality when the number of pixels is scaled up, will be addressed in the future paper.

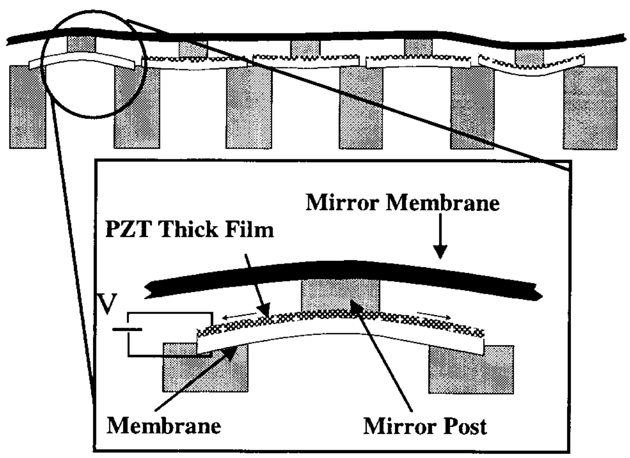

Figure 1 Thick film PZT based deformable mirror concept. A compliant, optical quality, single face-sheet mirror membrane is backed by an array of micro actuators. A voltage applied to the piezoelectric layer induces stress in the longitudinal direction causing the film to deform and pull on the mirror connected to it. The advantage of this approach is that the small strains obtainable from a piezoelectric material at modest voltages are translated into large displacements.

3. MODELING OF PZT UNIMORPH MEMBRANES

A modeling is performed for a unimorph membrane consisting of clamped rectangular membrane (area: 500 μm × 500 μm) with a PZT layer with variable dimensions. The modeling approach involves the following steps:

1. Selection of a functional form for the displacement vectors as a function of the coordinates.
2. Calculation of the resulting strain distributions.
3. Integration of the differential elastic and piezo-elastic energy contributions over the volume to obtain the total piezo-elastic energy
4. Minimized of this energy with some constraints (the displacements being zero along the membrane edge) to obtain the membrane profiles for the various PZT dimensions and applied voltages.

This procedure can be explained with a fairly text book approach below:

An absolute translation function is defined as a function of coordinates.

$$\xi_i(\vec{r}) = r_i + u_i(\vec{r}) \tag{1}$$

where r is the coordinate vector in 3D (x, y, z) and u is a vector function of coordinates corresponding to relative displacement of point (x, y, z). (i.e. point (x, y, z) moves to point (ξ_x, ξ_y, ξ_z))

The strain matrix is defined as follows.

$$\eta_{ij} = \frac{1}{2}(\frac{\partial u_i}{\partial r_j} + \frac{\partial u_j}{\partial r_i}) \tag{2}$$

Since the strain matrix has only 6 independent components due to symmetry considerations, a reduced strain vector can be defined as such.

$$\vec{\sigma} = \{\eta_{11}, \eta_{22}, \eta_{33}, 2\eta_{23}, 2\eta_{13}, 2\eta_{12}\} \tag{3}$$

Only the six independent components of the strain are included. The first three correspond to compressive/tensile strains in the x,y, and z directions, and the second three are the shear strains in the yx, xz, and xy planes respectively. The differential elastic energy (i.e., per unit volume) has the following form.

$$U_{el} = \vec{\sigma} \cdot \tilde{c} \cdot \vec{\sigma} = \sigma_i \cdot c_{ij} \cdot \sigma_j \tag{4}$$

where c_{ij} is the elastic coefficient matrix particular to the material. The piezoelectric contribution has the following form.

$$U_{pz} = \vec{\sigma} \cdot \tilde{e} \cdot \vec{E} = \sigma_i \cdot e_{ij} \cdot E_j \tag{5}$$

where e_{ij} is the piezoelastic coefficient matrix particular to the piezoelectric material (PZT) and E_j's are electric field vector components. These energy contributions for the materials are summed and integrated over the respective undeformed volumes in order to obtain the total piezoelastic energy.

$$U_{elastic} = \int_{V_{Silicon}} \sigma_i(\vec{r}) \cdot c_{ij}^{silicon} \cdot \sigma_j(\vec{r}) d^3r + \int_{V_{PZT}} \{\sigma_i(\vec{r}) \cdot c_{ij}^{PZT} \cdot \sigma_j(\vec{r}) + \sigma_i(\vec{r}) \cdot e_{ij}^{PZT} \cdot E_j\} d^3r \tag{6}$$

This energy is subsequently minimized to get the functional forms for $u_i(\vec{r})$'s. In order to simplify the calculations we make a number of simplifications to the otherwise fairly complex problem. The displacement functions are assumed as general polynomials with the forms given below.

$$\begin{aligned} u_x(x, y, z) &= u_x^0 + zu_x^1 = \sum_{j,i} (k_{ij}^0) x^i y^j + z\sum_{j,i} (k_{ij}^1) x^i y^j \\ u_y(x, y, z) &= u_y^0 + zu_y^1 = \sum_{j,i} (k_{ij}^0)(-x)^j y^i + z\sum_{j,i} (k_{ij}^1)(-x)^j y^i \\ u_z(x, y, z) &= \sum_{j,i} (k_{ij}^z) x^i y^j \end{aligned} \tag{7}$$

For the equations above, the same coefficients are used for u_x and u_y of the rectangular membrane, which has C_4 symmetry related by a 90° rotation. The u_x is odd in x and even in y, and the u_z is even in x and y. These considerations allow significant reduction of the number of k_{ij} coefficients. Since the membrane is thin, it is reasonable to assume that the shear strains are nearly zero. The coefficients are expressed as follows.

$$k_{ij}^1 \cong (i+1) k_{i+1,j}^z \tag{8}$$

There are two independent sets of coefficients, k_{ij}^{0} and $k_{ij}^{1} \cong (i+1)k_{i+1,j}^{z}$. A 24[th] order even power polynomial is selected for u_z and similar order polynomial is chosen for u_x and u_y, taking into account their symmetry (24[th] in the even variable and 23[rd] in the odd one). To obtain more realistic results a vertical strain for each layer was explicitly included by scaling the horizontal strains by the 2D Poisson's ratio,

$$\sigma_z = \frac{c_{12}}{c_{11}}(\sigma_x + \sigma_y) \tag{9}$$

for Si or Si_3N_4 and

$$\sigma_z = \frac{c_{13}}{c_{33}}(\sigma_x + \sigma_y) \tag{10}$$

for PZT. This choice of vertical strain explicitly minimizes the elastic energy locally for a membrane free in the vertical direction. The inclusion of this strain term corresponding to a quadratic term in z in the vertical displacement function compensates to a large extent for the difference in the Poisson's ratio of the two materials.

A set of constraints is included into the minimization calculation using the method of Lagrange multipliers. These constraints include both the membrane clamp conditions around the perimeter ($u_z(x=0$ or $y=0) = 0$) and the center displacement ($u_z(0 , 0) = h$). With the latter condition, the followings can be obtained:

a) Center displacement explicitly
b) Force for a constant displacement
c) Restoring force (the relevant Lagrange multiplier)

The total modified energy with the constraints included is therefore given as

$$U_{tot} = U_{elastic} + \sum_i l_i(f_i - h_i) \tag{11}$$

where l_i's are Lagrange multipliers, f_i are constraint functions (such as $u_z(0 , 0)$ in the case of the center displacement), and h_i's are the constraint values.

A set of linear equations for the polynomial coefficients and the Lagrange multipliers are generated by taking partial derivatives with respect to all the unknown coefficients (a standard constrained minimization approach)

$$\frac{\partial U_{tot}}{\partial c_i} = 0 \tag{12}$$

where c_i 's represent all the coefficients and the Lagrange multipliers to be solved for. The resulting system of linear equations is solved numerically to obtain the relevant coefficients for the membrane profiles and center-point displacements for various sets of initial conditions (such as the membrane dimensions, membrane thickness, materials properties, applied voltages, and normal forces). These coefficients are subsequently substituted into the original forms of the displacement function to obtain the membrane profiles.

3.1 Examples

A set of modeling is performed for a 500 μm × 500 μm supporting membrane (the non-piezo portion of the unimorph) clamped around the perimeter 500 μm × 500 μm. Three different membranes are considered; 16 μm thick Si, 26 μm thick Si, and 2 μm thick Si_3N_4. The intrinsic stress in single crystal silicon membranes and silicon nitride membranes are set to 0 and 100 Mpa, respectively. For these three cases, actuating electrode lateral dimensions and PZT thickness are varied in order to obtain optimal conditions for the maximum center displacement at a constant field (assumption: 10 kV/cm). A set of displacements versus normal force and applied voltage, with the optimized actuator, is calculated to characterize the actuator performance for driving non-zero loads. Figure 2 shows the displacements for various values of PZT dimensions and PZT thickness for the three cases. In each case, a roughly 500 μm × 500 μm electrode size is optimal, with the thickness comparable to that of the supporting membrane.

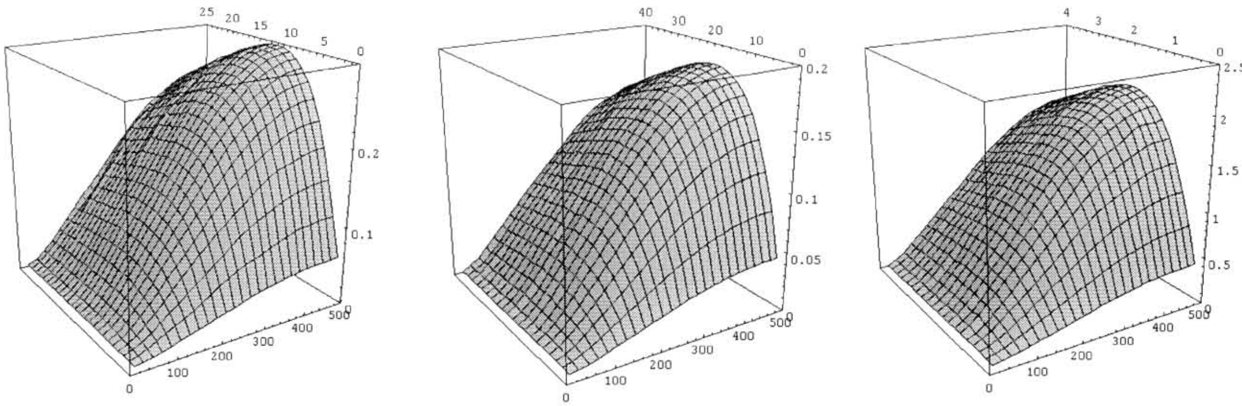

16 μm thick Si   26 μm thick Si   2 μm thick Si_3N_4

Figure 2. 3D and density plots of displacement vs. electrode lateral dimensions and the thickness. All numbers are in μm.

The optimal conditions are 500 μm × 500 μm × 12.1 μm thick PZT for the 16 μm thick Si support membrane, 500 μm × 500 μm × 19.7 μm thick PZT for the 26 μm thick Si support membrane, and 480 μm × 480 μm × 2.1 μm thick PZT for the 2 μm thick Si_3N_4 support membrane. Subsequently membrane deflections were calculated using these optimal parameters for the three membranes for various voltage and normal force conditions. These results are presented below

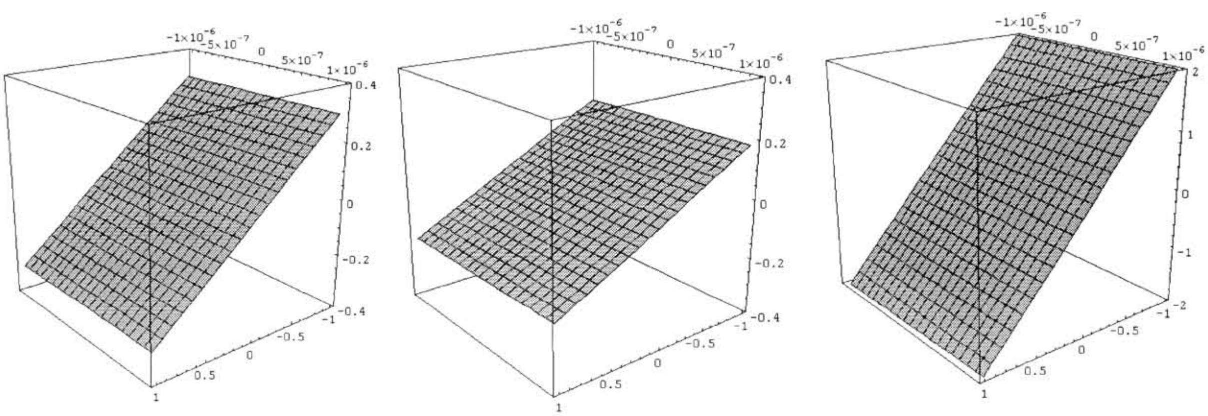

16 μm thick Si   26 μm thick Si   2 μm thick Si_3N_4

Figure 3. 3D and density plots of displacement vs. applied voltage (V vs. μm) and normal force (N).

4. FABRICATION AND CHARACTERIZATION OF MIRROR MEMBRANE

4.1 Membrane transfer technology

From our literature survey, none of the existing technologies can meet all of the demanding requirements of optical quality, mechanical compliance and pixel density required for high spatial frequency deformable mirrors. The advanced processing technology developed at JPL for transferring an optical quality membrane over an actuator array is to meet these requirements for a MEMS-based continuous membrane deformable mirror. Microfabricated membranes often show warping or wrinkling due to the intrinsic stress or the stress generated during the bonding and etching processes. However, previous work by our group resulted in the successful demonstration of a micromachined membrane without observable warping [9]. In this previous work, the wafer with the transferred silicon plate was diced into small pieces (surface area of 5 mm^2) prior to completing the transfer process to implement electrostatic actuator arrays with pixel-to-pixel spacing of 200 μm. Figure 5 shows the SEM photographs of transferred polysilicon actuators. An optically polished silicon wafer is used as a carrier wafer, and a flexible mirror membrane material is subsequently deposited. An optical quality membrane deformable mirror can be obtained by using a membrane material with an *intrinsic tensile stress - deposited on an optically polished carrier wafer*, essentially making the transferred membrane surface a replica of the surface of the carrier wafer.

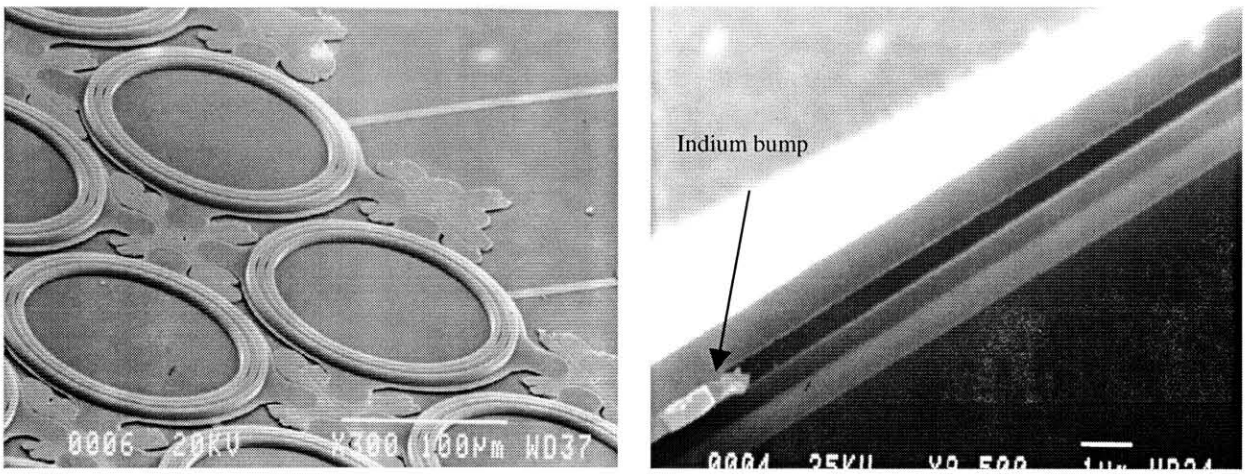

Figure 5 The SEM images of the 1 μm thick transferred polysilicon actuator [9].
(a) Fabricated electrostatic actuator array (b) Cross-sectional view

4.2 Thick film PZT technology

The deposition and patterning technologies of PZT thick films for integration into MEMS devices have been developed by a number of groups [10, 11]. High quality films can be uniformly deposited on 4" wafers using a sol-gel process by spin-coating the precursor solution onto platinum coated bottom electrodes. These films have been utilized in a number of MEMS devices, including an accelerometer and a number of diaphragm and cantilever actuators. On existing diaphragm structures with diameters of 500 μm, center deflections of >3 microns have been achieved using comparatively thin PZT films (~1.5 μm). For the larger stroke actuators, thicker PZT films would be utilized. Incorporating the thicker PZT films allows significant increase in the actuation stroke and force of the device.

4.3 Optical quality membrane mirror characterization

Figure 6 shows the local surface figure of a patterned 16μm thick silicon membrane after wafer-scale transfer, measured by using a WYKO interferometer. The transferred membrane shows the peak-to-valley surface figure error of 9 nm across the area of 2 mm^2. In this paper, several membrane materials including polymers will be tested in order to obtain the optical quality and mechanical compliance requirements. The fabricated mirror membrane will be characterized with a full aperture measurement, which allows for Michelson interferometry. A helium-neon laser will be used with a 50% reflectivity beam splitter. Figure 7 gives experimental setup for characterizing transferred mirror. When interferometry is performed on the membrane mirror surface, the beam reflecting off an optical flat interferes with the beam from the transferred mirror on a CCD.

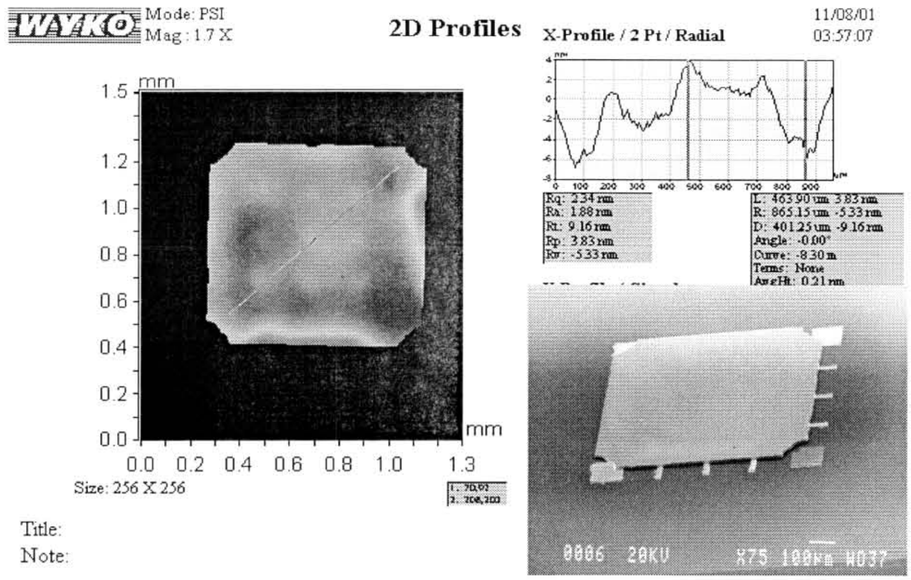

Figure 6 The surface figure of a transferred membrane. The surface figure error was 9 nm P-V for this sample.

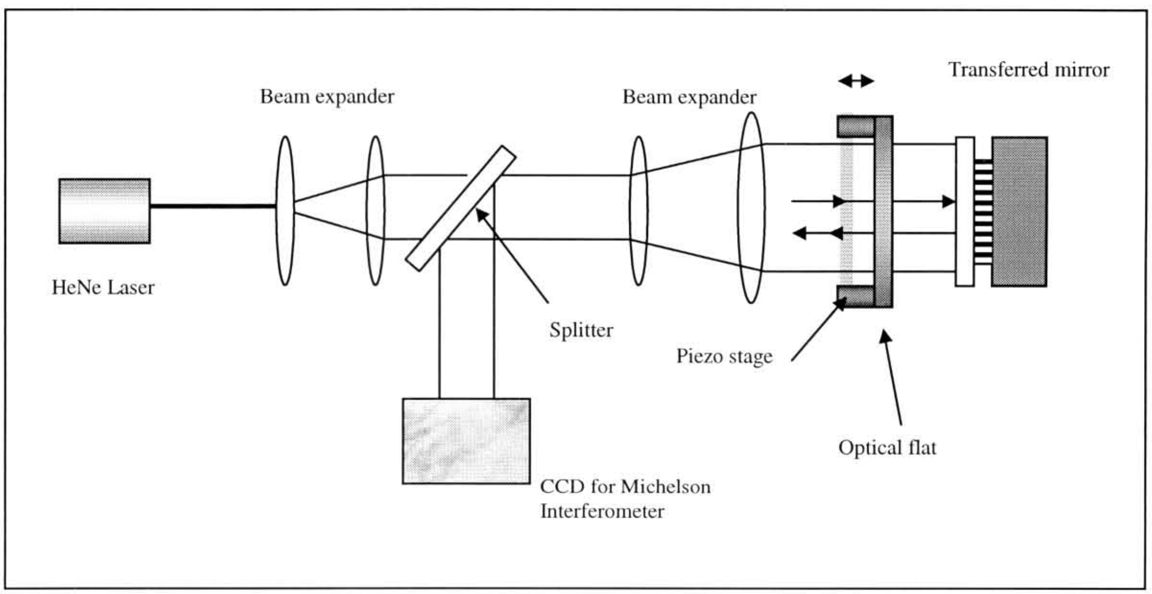

Figure 7 The experimental setup for testing transferred mirror that allows for Michelson interferometry.

Potential applications for the JPL MEMS deformable mirror technology in addition to space telescopes include:

(a) Reduced transmitter power requirements for long distance space-to-space or space-to-ground optical communications links

(b) Very large, non-optical (e.g. A cost-effective array of high bandwidth communication stations in geosynchronous orbit.), space based apertures fabricated using Silicon telescope technology

(c) Imaging the human retina at high resolution as a biometric signature for security purposes using a very compact, portable device. Although the turbulence structure of the human eye requires only 5-10 Hz closed-loop bandwidth correction, very large numbers of actuators are required for diffraction-limited operation.

5. CONCLUSION

The design and modeling of a piezoelectric unimorph deformable micromirror are presented. The deformable mirror device consists of a "transferred" continuous membrane mirror supported by individually moving actuators. This approach allows for other actuation mechanisms (e.g. such as conventional actuators) to be integrated with the membrane transfer technology. Thick film PZT concept is utilized for use in the high-density unimorph actuators. A set of modeling is performed for a 500 μm × 500 μm supporting membrane (the non-piezo portion of the unimorph) clamped around the perimeter 500 μm × 500 μm. A set of displacements versus normal force and applied voltage, with the optimized actuator, is calculated to characterize the actuator performance for driving non-zero loads. The optimal conditions are 390 μm × 390 μm × 13 μm thick PZT for the 16 μm thick Si support membrane, 390 μm × 390 μm × 20 μm thick PZT for the 26 μm thick Si support membrane, and 410 μm × 410 μm × 1.7 μm thick PZT for the 2 μm thick Si_3N_4 support membrane.

The success of the proposed technology will result in the development of a high-density deformable mirror technology with an optical quality surface figure. This mirror transfer technology could be combined with actuator devices with different specifications, tailored to a wide variety of optical systems needed for future space science missions ranging from the imaging of planets around other stars, to the search for life as embodied in NASA's Origins Program. This technology will reduce the volume and mass of a pixel by more than two-orders-of-magnitude, which will promote the design of smaller optical systems by a factor roughly proportional to the pixel size, while delivering a high quality, compact energy efficient system. The proposed technology will also benefit other missions that require miniature precision devices in a broad range of operational environments such as ground based telescopes and high precision imaging systems.

ACKNOWLEDGEMENTS

The research described in this paper was carried out by the Jet Propulsion Laboratory, California Institute of Technology under a contract with the National Aeronautics and Space Administration.

REFERENCES

1. M. A. Ealey and J. F. Washeba, "Continuous face sheet low voltage deformable mirrors," *Optical Eng., (29)* p.1191, Oct. 1990.
2. V.M.Bright et al., "Surface micromachined micro-opto-electro-mechanical systems," *IEICE Trans. Electron., vol. E80-C., No. 2,* pp. 206-213, Feb. 1997.
3. M. A. Michalicek et al., "Design and simulation of advanced surface micromachined micro mirror devices for telescope adaptive optics applications," *SPIE Conf. On Adaptive Optical System Technology*, Kona, Hawaii, March 1998, pp. 805-815.
4. W.D.Cowan et al., "Evaluation of microfabricated deformable mirror systems," *SPIE Conf. On Adaptive Optical System Technology*, Kona, Hawaii, March 1998, pp. 790-804.
5. G. Vdovin, "Optimization-based operation of micromachined deformable mirrors," *SPIE Conf. On Adaptive Optical System Technology*, Kona, Hawaii, March 1998, pp. 902-909.
6. P.K.C. Wang, et al., "A method for designing electrostatic-actuator electrode pattern in micromachined deformable mirrors," *Sensors and Actuators A, Vol. 55*, pp.211-217, 1996.
7. T. Bifano et al., "Continuous-membrane surface-micromachined silicon deformable mirror," *Opt. Eng. 36(5)*, p.1354 May 1997.
8. J. Mansell et al., "Silicon Deformable Mirrors and CMOS-based Wavefront Sensors," *SPIE International Conference, High-Resolution Wavefront Control*, San Diego, USA, 1-2 August, 2000, pp. 15-25.
9. E. H. Yang and Dean V. Wiberg, "A New Wafer-Level Membrane Transfer Technique for MEMS Deformable Mirrors," *IEEE MEMS 2001 Conference*, Switzerland, 2000, pp. 80-83.
10. L.-P. Wang, K. Deng, L. Zou, R. Wolf, R. J. Davis, and S. Trolier-McKinstry, "Microelectromechanical Systems (MEMS) Accelerometers Using Lead Zirconate Titanate Thick Films," *IEEE Electron Device Letters 23 (4)*, 182 – 184 (2002).
11. L-Peng Wang, *Ph.D. thesis*, the Pennsylvania State University, 2001

End of File